Published by Elsevier Inc.

ISSN 0735-1097/04/$30.00
doi:10.1016/j.jacc.2004.08.033

Global Impairment of Brachial, Carotid, and Aortic Vascular Function in Young Smokers

Direct Quantification by High-Resolution Magnetic Resonance Imaging

Frank Wiesmann, MD, Steffen E. Petersen, MD, Paul M. Leeson, MD, Jane M. Francis, DCR, Matthew D. Robson, PHD, Qian Wang, MD, Robin Choudhury, MD, Keith M. Channon, MD, FRCP, Stefan Neubauer, MD, FRCP

Oxford, United Kingdom

OBJECTIVES The purpose of this study was to assess vascular dysfunction in young smokers by high-resolution magnetic resonance imaging (MRI).

BACKGROUND Cigarette smoking is a well-known cause of endothelial dysfunction, reflected by impaired brachial artery reactivity to hyperemia. We hypothesized that smoking induces both peripheral endothelial dysfunction and altered function in central conduit arteries, and that these global changes in vascular function could be directly quantified in a single noninvasive examination using high-resolution MRI.

METHODS A total of 22 healthy young volunteers (mean age 31 ± 2 years; 12 nonsmokers, 10 smokers: cumulative cigarette consumption 11.9 ± 6.0 pack-years) underwent noninvasive high-resolution MRI to assess central vascular distensibility and pulse-wave velocity (PWV), and cross-sectional flow-mediated dilation (FMD) of the brachial artery.

RESULTS Brachial artery FMD was significantly reduced in smokers compared with nonsmokers (7.5 ± 2.7% vs. 15.5 ± 2.0%; $p = 0.03$), indicating impaired endothelium-dependant relaxation, whereas endothelium-independent responses to sublingual glyceroltrinitrate (400 μg) were identical in both groups. Impaired peripheral endothelial function in smokers was accompanied by striking decreases in central vascular distensibility in both the common carotid arteries (−45.7%; $p = 0.02$) and at multiple sites in the aorta (ascending aorta −26.9%, $p = 0.04$; thoracic descending aorta −25.0%, $p = 0.01$; abdominal descending aorta −25.5%, $p = 0.02$). Aortic arch PWV in smokers was increased by 19% ($p = 0.02$).

CONCLUSIONS Cigarette smoking induces global changes in both peripheral and central vascular function. Direct quantification of multiple parameters of vascular function using high-resolution MRI will provide powerful new approaches to the assessment of vascular disease pathogenesis, diagnosis, and treatment. (J Am Coll Cardiol 2004;44:2056–64) © 2004 by the American College of Cardiology Foundation

Endothelial dysfunction is a cardinal feature of vascular disease states such as atherosclerosis (1) and is associated with an increased risk for cardiovascular events (2,3). Moreover, endothelial dysfunction in the peripheral vasculature is an independent predictor of future cardiovascular events in patients with either established cardiovascular disease or with risk factors for vascular disease development (4–6). These findings suggest that endothelial dysfunction reflects biological changes in the vasculature that confer poor cardiovascular prognosis.

Despite this established association between endothelial dysfunction and cardiovascular events, little is known about the relationship between impaired peripheral endothelial function and the contribution of the endothelium and other vessel wall components to the regulation of central arterial distensibility (7). Indeed, vascular disease is associated with changes in many other indexes of vascular function, including conduit artery distensibility and pulse-wave velocity (PWV). Flow-mediated dilation (FMD), a nitric oxide-mediated endothelial response, is typically assessed by ultrasound techniques. However, FMD measured by ultrasound is sometimes limited by low resolution and high variability that substantially impair statistical power. Accordingly, there is continuing interest in the development of improved noninvasive approaches to endothelial function studies. Furthermore, the need for more global and sophisticated approaches to vascular phenotyping is highlighted by recent studies suggesting that further measures of vascular function such as arterial stiffness provide important additional information in refining cardiovascular risk in medium- or low-risk subjects (8,9). These novel parameters may be particularly useful in identifying individual patients who will benefit from certain therapeutic strategies, or in quantifying the response to a therapeutic or lifestyle intervention.

From the University of Oxford Centre for Clinical Magnetic Resonance Research, Department of Cardiovascular Medicine, University of Oxford, Oxford, United Kingdom. Supported by grants from the Wellcome Trust (Intermediate Research Fellowship to Dr. Wiesmann) and by the British Heart Foundation (Drs. Neubauer and Channon), the German Academic Exchange Service (Dr. Petersen), and the Deutsche Forschungsgemeinschaft (Dr. Wiesmann).

Manuscript received May 3, 2004; revised manuscript received July 4, 2004, accepted August 9, 2004.

Abbreviations and Acronyms

AA = ascending aorta
DDA = distal descending aorta
FMD = flow-mediated dilation
MRI = magnetic resonance imaging
PWV = pulse-wave velocity

Magnetic resonance imaging (MRI) bears great potential in evaluating vascular anatomy and function due to its high temporal and spatial resolution. The use of different MRI techniques optimized for angiography (10–12), assessment of vascular elasticity (13–15), and quantification of luminal and vessel wall parameters (16–18) allows for a comprehensive and detailed view of the vascular system.

In this study, we developed high-resolution MRI techniques to noninvasively quantify both peripheral endothelial dysfunction and central conduit artery function in a single examination. We evaluated the utility of this approach to investigate the effects of cigarette smoking on global vascular function in young healthy volunteers.

METHODS

Study participants. Twenty-two young healthy volunteers were enrolled in this study. Of these, 10 subjects (mean age 31 ± 2 years) were active smokers (average daily cigarette consumption 9.3 ± 4.2 /day; cumulative nicotine consumption 11.9 ± 6.0 pack-years). Twelve healthy volunteers without any history of smoking acted as control group. Neither smokers nor nonsmokers had received any vasoactive medication before or at inclusion. Subjects were excluded if any of the following factors known to cause endothelial dysfunction were present: hypertension, coronary artery disease, dyslipidemia, overweight and obesity (body mass index >25), or a family history of premature coronary artery or cerebrovascular disease. Characteristics of the study population are shown in Table 1.

The study was approved by the local research ethics committee, and all subjects gave written informed consent.

MRI technique. Magnetic resonance imaging was performed on a 1.5-T clinical magnetic resonance scanner (Siemens Sonata, Erlangen, Germany) with subjects in the supine position. For aortic imaging, a combination of a two-element-array surface coil placed on the chest and a spine-coil-array within the patient bed was used. Carotid artery imaging was performed using a two-element-array surface coil (Machnet BV, Eelde, The Netherlands). For brachial artery imaging, a flexible surface coil was attached to the right elbow (Fig. 1).

Table 1. Characteristics of Study Participants

	Smokers (n = 10)	Nonsmokers (n = 12)
Age (yrs)	31 ± 2	31 ± 2
Male/female	5/4	6/5
Height (cm)	176 ± 3	171 ± 2
Weight (kg)	71.9 ± 3.3	66.7 ± 2.7
Body surface area (mm^2)	1.81 ± 0.75	1.79 ± 0.57
Systolic blood pressure (mm Hg)	115 ± 4	112 ± 4
Diastolic blood pressure (mm Hg)	67 ± 3	72 ± 3
Mean blood pressure (mm Hg)	83 ± 3	85 ± 3
Pulse pressure (mm Hg)	48 ± 4*	39 ± 2
Heart rate (beats/min)	61 ± 2	65 ± 3

*$p < 0.05$ vs. nonsmokers. Values are mean ± SEM.

Vascular distensibility of the aorta and common carotid arteries was assessed using a TrueFISP (fast imaging with steady state free precession) cine sequence with the following parameters: aorta repetition time/echo time (TR/TE) 42 ms/1.4 ms, field of view in read direction (FOV_{read}) 380 mm, in-plane resolution 1.97 mm, slice thickness 7 mm, and carotid TR/TE 45.3 ms/2.4 ms, FOV_{read} 200 mm, in-plane resolution 0.52 mm, and slice thickness 3 mm (for aortic and carotid cine videos, please see the November 16, 2004, issue at www.onlinejacc.org.).

The imaging position for the brachial artery was chosen from a three-dimensional angiographic pilot scan in order to align the imaging plane perpendicular to the artery. Cross-sectional area of the brachial artery was measured by manual delineation of inner vessel boundaries using CMR tools image post-processing software (developed by Imperial College, University of London, United Kingdom). Validation of this software-based assessment of brachial artery reactivity has been described previously in more detail (19). Magnetic resonance measurement of brachial artery area was performed at baseline and 1 min after reactive hyperemia was induced by release of a forearm cuff inflated to suprasystolic pressure for 4.5 min. For assessment of endothelial-independent brachial artery dilation, magnetic resonance data acquisition was repeated before and 3 min after sublingual application of 400 μg glyceroltrinitrate. Cardiac-gated TrueFISP cine images of the brachial artery were acquired with the following parameters: TR/TE 56/3 ms, flip angle 66°, FOV 117 × 77 mm, matrix 384 × 252, 16 segments, 11 to 19 phases depending on heart rate (Fig. 1).

For aortic distensibility and flow measurements, sagittal-oblique pilot images were acquired aligned with the aortic arch (Fig. 2). A high-resolution gradient-echo pulse sequence with a velocity-encoding gradient for phase-contrast MRI was applied with TE 2.8 ms, effective TR 1 RR-interval, flip angle 30°, matrix size 256 × 192, FOV 320 × 240 mm, slice thickness 5 mm, temporal resolution 11 ms per cine frame. Flow measurements in the aorta were made at three levels: the crossing of the pulmonary artery through: 1) the ascending aorta (AA); and 2) the descending aorta; and 3) at a level approximately 10 cm below the diaphragm. Distances between the levels were measured on the magnetic resonance scanner console from the scout images of the aortic arch.

Blood pressure was measured from the left arm using a brachial artery sphygmomanometer during distensibility measurements of the aorta and carotid arteries and during

JACC Vol. 44, No. 10, 2004
November 16, 2004:2056–64

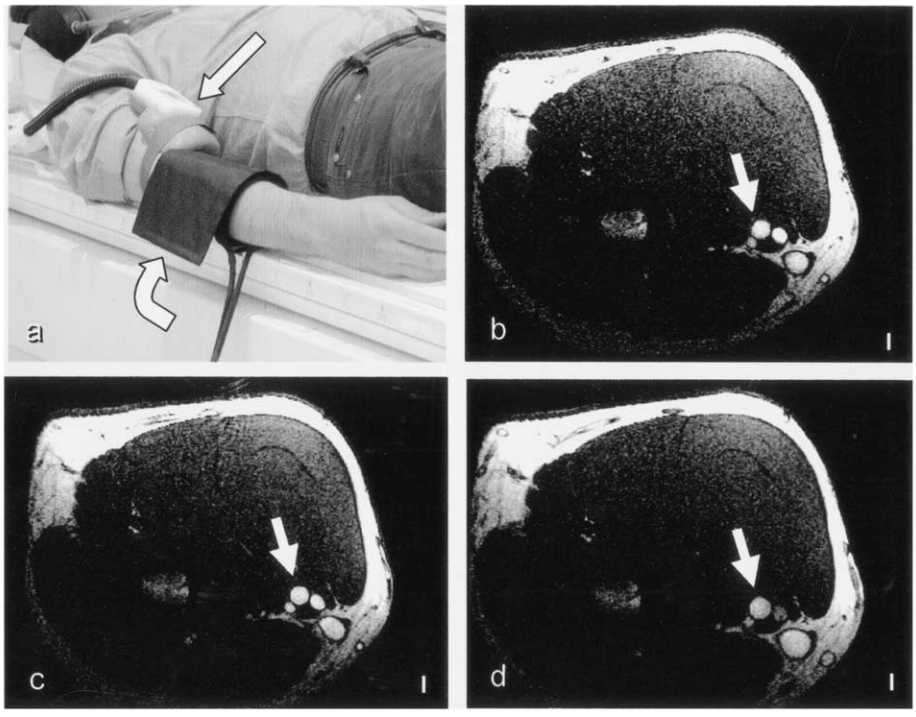

Figure 1. Magnetic resonance imaging (MRI) of brachial artery reactivity to hyperemia. **(a)** Set up for brachial artery imaging in the magnetic resonance scanner with a pressure cuff on the forearm distal to the imaging site **(curved arrow)** and a surface coil placed above the elbow region for optimal magnetic resonance signal detection **(straight arrow)**. **(b to d)** High-resolution MRIs aligned perpendicular to the brachial artery **(arrows)**. **(b)** Baseline conditions (**scale bar** = 3 mm). Note the increase in brachial artery cross-section area **(c)** 1 min after cuff release (representing flow-mediated dilation) and **(d)** 3 min after GTN application (endothelium-independent relaxation).

brachial artery imaging. To exclude confounding effects on endothelial function, MRI was performed after a minimum of 20 min sitting-rest and at a constant room temperature of 20°C. Magnetic resonance imaging with switching between different coil array systems during the study could be performed and successfully completed in all 22 subjects

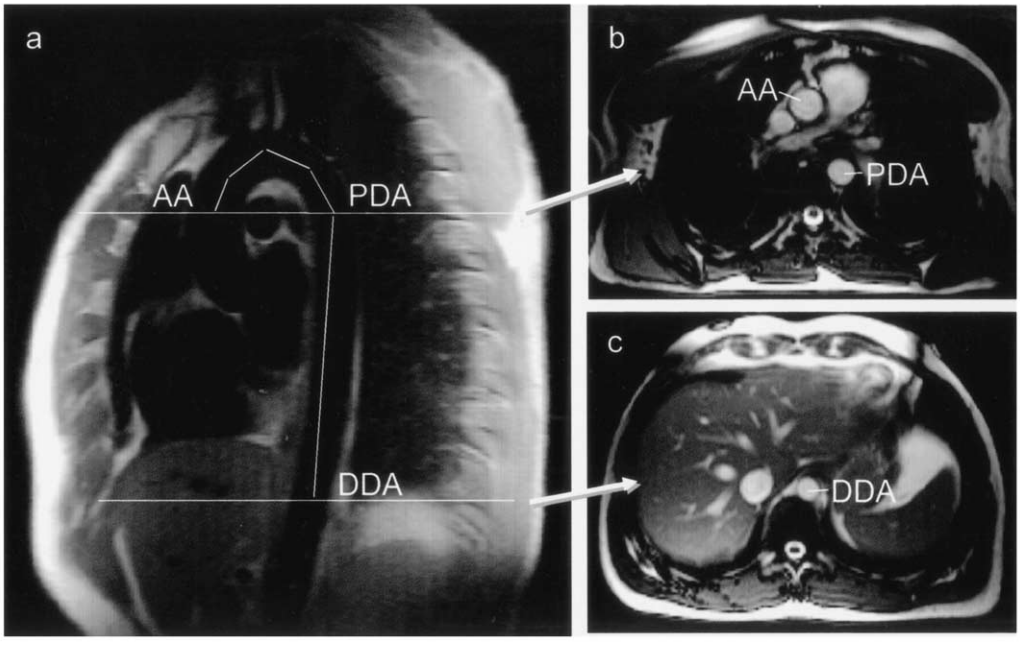

Figure 2. **(a)** Coronal-sagittal oblique scout image aligned with the aortic arch and descending aorta for assessment of distances between measurement points. Distance evaluation between the ascending aorta (AA) and proximal descending aorta (PDA) was performed by a series of **short straight connected lines** along the aortic luminal midline in the curved aortic arch, because the software did not allow for curved measurements. Distance between PDA and distal descending aorta (DDA) was assessed by a single-line measurement. **Panels (b) and (c)** show the corresponding TrueFISP images in transverse orientation.

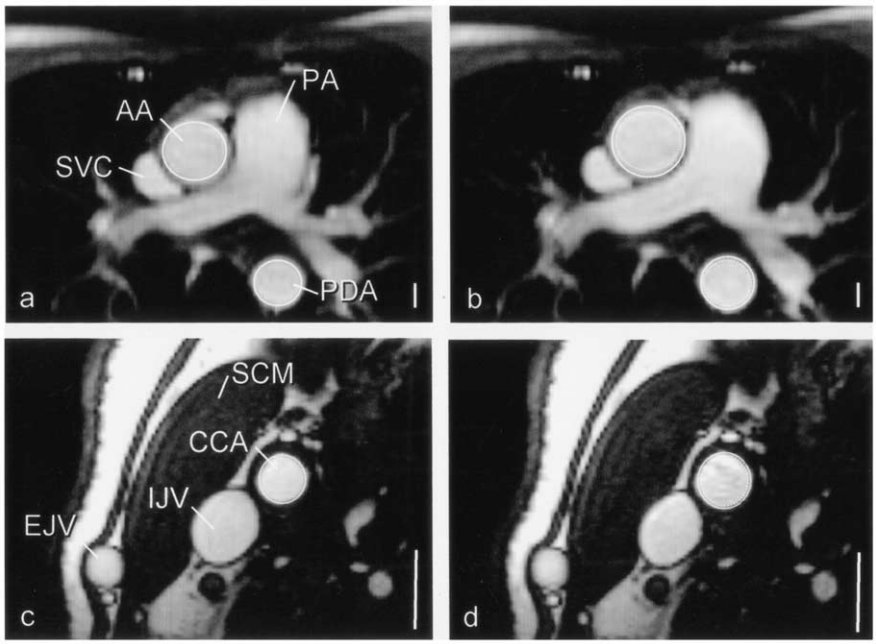

Figure 3. Magnetic resonance imaging (MRI) of central vascular compliance. Vessel wall tracings in transverse CINE TrueFISP MRIs acquired at the level of the pulmonary artery (PA) bifurcation revealing cross-section through the ascending (AA) and proximal descending aorta (PDA) at **(a)** diastole and **(b)** systole. **(c and d)** The MRIs of the right common carotid artery (CCA) acquired at diastole and systole. Note the increase in vessel cross-sections at systole **(solid ellipse in b and d)** in comparison with corresponding diastolic cross-sections **(dotted ellipse in b and d)**. All images are cropped for display purposes (**scale bar** = 10 mm). EJV = external jugular vein; IJV = internal jugular vein; SCM = sternocleidomastoid muscle; SCV = superior vena cava.

studied. High-resolution MRIs were of high quality and were suited for quantitative analysis in all subjects.

Data analysis. All data analysis was performed in a blinded fashion after removal of identity information from the original MRIs. For evaluation of vascular distensibilities, inner boundaries of the aortic, carotid, and brachial artery walls were traced manually (Fig. 3). Vascular distensibility (mm Hg^{-1}) was calculated as relative change in cross-sectional area for a given pressure change according to the formula: Distensibility = $(A_{max} - A_{min})/A_{min} \cdot (P_{max} - P_{min})$, where A_{max} = maximal (systolic) area (mm^2), A_{min} = minimal (diastolic) area (mm^2), P_{max} = systolic blood pressure (mm Hg), and P_{min} = diastolic blood pressure (mm Hg) (9).

Flow measurements were performed with Argus Software (Siemens, Erlangen, Germany). The distance between the measurement points across the aortic arch was measured manually on the double-oblique scout image visualizing the course of the thoracic aorta. Distance measurement was done manually by a series of short straight connected lines along the aortic luminal midline (Fig. 2), because the post-processing tool did not allow for freehand line drawing. Assessment of distance between measurement points in the proximal and distal descending aorta (DDA) was done by a single line. The PWV (m/s) was calculated by dividing the distance between measurement levels by time difference between arrival of the pulse wave at these levels. Arrival time of the pulse wave at each level was defined as the time point when the mean velocity reached half of its maximum value (20). A straight line fit (minimum least squares) to the five velocity data points nearest to the half maximum point was performed using Origin (Software Version 7, OriginLab Corp., Northhampton, Massachusetts), and the intersection of this line with the half maximum was determined, which enables arrival time determination at higher temporal resolution than the imaging resolution. Reproducibility of measurements was assessed by repeated magnetic resonance data analysis in the 12 control subjects. Twenty subjects also underwent ultrasound evaluation of brachial artery reactivity using standard methods (21) based on high-resolution ultrasound imaging (Philips Sonos 5500 and vascular probe, Best, The Netherlands) and automated image analysis (Vascular Analyser, Medical Imaging Applications, Iowa City, Iowa).

Statistical analysis. Statistical analysis was performed using StatView (Software Version 5, SAS Institute Inc., Cary, North Carolina). All results are expressed as mean values ± SEM unless otherwise specified. For assessment of functional differences between smokers and control subjects, an unpaired Student *t* test was performed. Simple linear regression was used to determine the relationship between measured parameters. A value of $p < 0.05$ was considered significant.

RESULTS

Patient characteristics. There were no differences in mean age, gender distribution, height, or weight between smokers and nonsmoking control subjects (Table 1). Furthermore, blood pressure recordings during the magnetic resonance

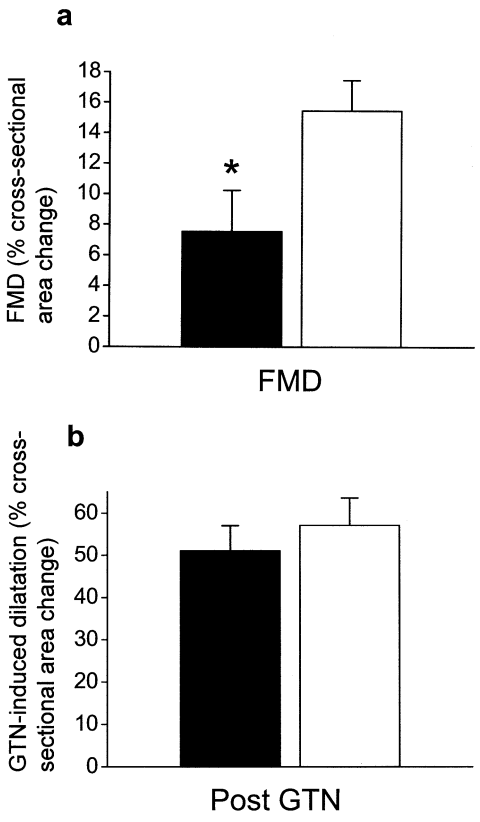

Figure 4. Relative cross-sectional area changes induced by **(a)** hyperemia (flow-mediated dilation [FMD] representing endothelium-dependent relaxation) and by **(b)** GTN (endothelium-independent relaxation) in 10 smokers and 12 nonsmokers. **Solid bars** = smokers; **open bars** = controls. *$p < 0.05$.

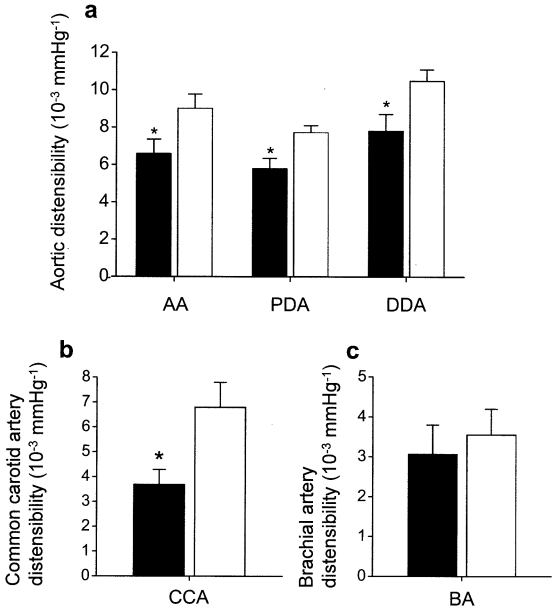

Figure 5. Comparison of vascular distensibility between young smokers and control subjects quantified by magnetic resonance imaging at **(a)** different sites of the aorta, **(b)** in the common carotid artery, and **(c)** in the brachial artery. AA = ascending aorta; BA = brachial artery; CCA = common carotid artery; DDA = distal descending aorta; PDA = proximal descending aorta. **Solid bars** = smokers; **open bars** = controls. *$p < 0.05$.

exam revealed similar systolic and diastolic blood pressure, mean blood pressure, and heart rate in both groups. However, calculation of pulse pressure resulted in a significantly higher value in the smokers (48 ± 4 mm Hg vs. control 39 ± 2 mm Hg; $p = 0.037$).

Brachial artery FMD and GTN response. Mean baseline brachial artery cross-sectional areas acquired at end-diastole were similar in smokers and control subjects (12.7 ± 1.2 mm^2 vs. control 12.1 ± 1.4 mm^2; $p = 0.74$). Hyperemia-induced dilation of the brachial artery was significantly reduced in smokers compared with the control group, expressed as both absolute cross-sectional area changes (0.93 ± 0.38 mm^2 vs. control 1.69 ± 0.18 mm^2; $p < 0.05$) and for relative area changes (7.53 ± 2.71% vs. control 15.45 ± 2.00%; $p < 0.05$), indicating impaired endothelial-dependent brachial artery dilation in the young smokers (Fig. 4). However, brachial artery reactivity to GTN was similar for both groups (absolute change 6.17 ± 0.58 mm^2 vs. control 6.69 ± 0.56 mm^2, $p = 0.53$; relative change 51.05 ± 5.95% vs. control 57.05 ± 6.51%, $p = 0.48$). Hence, nitric oxide-mediated, endothelium-independent relaxation of peripheral vascular smooth muscles and dilation of brachial arterial wall was unchanged in smokers compared with the nonsmokers.

Aortic, carotid, and brachial artery distensibility. Comparison of cross-sectional areas at different sites of the aorta acquired at diastole showed no significant differences between smokers and controls in either the AA (464.4 ± 37.0 mm^2 vs. control 428.5 ± 28.9 mm^2; $p = 0.44$), the proximal descending aorta (285.4 ± 18.3 mm^2 vs. control 257.9 ± 14.9 mm^2; $p = 0.25$), or in the DDA (200.2 ± 15.7 mm^2 vs. control 181.8 ± 10.1 mm^2; $p = 0.32$). The progressive decrease in aortic dimension toward the distal aorta was similar in both groups. Magnetic resonance quantification of aortic distensibility revealed a significant decrease in smokers compared with controls in all sites: AA (6.59 ± 0.77 10^{-3} mm Hg^{-1} vs. control 9.01 ± 0.77 10^{-3} mm Hg^{-1}; $p < 0.05$), proximal thoracic descending aorta (5.79 ± 0.55 10^{-3} mm Hg^{-1} vs. control 7.72 ± 0.38 10^{-3} mm Hg^{-1}; $p < 0.01$), and abdominal aorta (7.81 ± 0.90 10^{-3} mm Hg^{-1} vs. control 10.49 ± 0.61 10^{-3} mm Hg^{-1}; $p < 0.03$) (Fig. 5).

There was no difference of common carotid area dimensions acquired both in diastole (32.3 ± 2.0 mm^2 vs. control 35.7 ± 3.5 mm^2; $p = 0.42$) and systole (38.0 ± 2.9 mm^2 vs. control 44.7 ± 3.3 mm^2; $p = 0.15$) between smokers and nonsmokers. However, common carotid artery distensibility was significantly reduced in the smoker group (3.69 ± 0.60 10^{-3} mm Hg^{-1} vs. 6.80 ± 1.00 10^{-3} mm Hg^{-1}; $p = 0.02$) (Fig. 5b).

In contrast with findings in aorta and carotid arteries, brachial artery cross-sectional area changes within the cardiac cycle revealed similar brachial artery distensibility in

Table 2. Comparisons of Blood Volume Flow, Blood Velocity, and Pulse Wave Velocity Between Young Smokers and Healthy Controls

	Smokers (n = 10)	Nonsmokers (n = 12)	p Value
Aortic forward flow (ml)	54.8 ± 4.5	51.9 ± 4.0	0.63
Aortic reversed flow (ml)	3.11 ± 0.65	3.31 ± 0.80	0.85
Aortic net flow (ml)	51.6 ± 4.6	48.5 ± 3.8	0.60
Aortic flow output (l/min)	3.23 ± 0.24	3.29 ± 0.16	0.84
Peak blood velocity AA (m/s)	103.3 ± 7.3	104.8 ± 5.6	0.87
Peak blood velocity PDA (m/s)	122.0 ± 4.6	118.1 ± 5.0	0.57
Peak blood velocity DDA (m/s)	98.4 ± 7.0	98.6 ± 5.0	0.98
Proximal PWV (m/s)	5.24 ± 0.29	4.41 ± 0.16	0.02
Distal PWV (m/s)	4.75 ± 0.32	4.77 ± 0.32	0.96

Values are mean ± SEM.
AA = ascending aorta; DDA = distal descending aorta; PDA = proximal descending aorta; PWV = pulse-wave velocity.

both groups studied (smokers 3.06 ± 0.74 10^{-3} mm Hg^{-1} vs. control 3.55 ± 0.65 10^{-3} mm Hg^{-1}; p = 0.62) (Fig. 5c).

Aortic blood flow and PWV. Comparison of aortic forward flow, reversed flow, and aortic net flow showed no differences between smokers and controls (Table 2). Furthermore, aortic flow output was similar in both groups (3.23 ± 0.24 l/min vs. 3.29 ± 0.16 l/min; p = 0.84). Magnetic resonance-derived aortic peak velocities during the cardiac cycle were unchanged in smokers for measurements performed in the AA, proximal descending aorta, and DDA (p = 0.87, p = 0.57, and p = 0.98, respectively). However, evaluation of aortic PWV revealed an increased velocity in the proximal aorta comprising AA and aortic arch in the smokers (5.24 ± 0.29 m/s vs. 4.41 ± 0.16 m/s; p = 0.02). Distal PWV in the descending aorta was not different between the groups (4.75 ± 0.32 m/s vs. 4.77 ± 0.32 m/s; p = 0.96).

Correlation of magnetic resonance measurements. Comparison of pulse pressure with aortic distensibility showed highest inverse correlation for the most distal aortic measurement site (r = −0.74) with lower correlation coefficients for more proximal sites at the proximal descending aorta (r = −0.57) and the AA (r = −0.49; p < 0.001 each). Regression analysis for flow-mediated brachial artery dilation with aortic distensibility at the three measurement levels revealed no significant correlation (r = 0.10 each for AA, proximal descending aorta, and DDA). Furthermore, both proximal and distal aortic pulse-wave velocities correlated only weakly with regional aortic distensibility: proximal PWV showed highest correlation with AA distensibility (r = 0.20) with lower correlation for proximal descending aorta and DDA distensibility (r = 0.03 and r = 0.11; p < 0.0001 each). The PWV in the descending aorta correlated best with aortic distensibility in the thoracic descending aorta (p = 0.30) and relatively lower with AA and proximal descending aorta distensibility (r = 0.17 and r = 0.23; p < 0.0001 each).

Reproducibility of measurements. Repeated measurements of brachial artery cross-sectional area at baseline and after cuff release showed close agreement with mean differences (± standard deviation of two measurements) of −0.11 ± 0.56 mm^2 and 0.03 ± 0.76 mm^2, resulting in coefficients of variability of 0.05 and 0.06, respectively. Comparison of FMD from two measurements revealed a mean difference of 0.75 ± 4.80% (coefficient of variability 0.32). Furthermore, repeated evaluation of mean differences of aortic distensibility in the AA (0.43 ± 1.49 10^{-3} mm Hg^{-1}), proximal descending aorta (0.02 ± 1.47 10^{-3} mm Hg^{-1}), and DDA (0.04 ± 2.27 10^{-3} mm Hg^{-1}) showed close agreement with coefficients of variability of 0.18, 0.23, and 0.23, respectively. Similarly, there was only a small difference between measurements for carotid artery distensibility (0.04 ± 1.07 10^{-3} mm Hg^{-1}), resulting in a coefficient of variability of 0.19. Repeated analysis of aortic PWV revealed a difference of −0.09 ± 0.67 m/s for the proximal aorta and −0.13 ± 0.80 m/s for the distal aorta with corresponding coefficients of variability of 0.14 and 0.16, respectively.

Comparison of MRI to ultrasound. Brachial artery diameters measured by ultrasound were strongly correlated with brachial artery cross-sectional areas measured by MRI (r = 0.83, p < 0.001 at baseline and r = 0.82, p < 0.001 after forearm cuff occlusion). The mean difference between brachial artery cross-sectional areas calculated from ultrasound assessment of diameter and cross-sectional MRI images was 1.1 ± 0.6 mm^2. Flow-mediated dilation measured by ultrasound and MRI was correlated (r = 0.62; p = 0.01) even though measures by the two modalities were several days apart. Mean difference in FMD within individuals, measured by the two techniques, based on change in cross-sectional area was −0.16 ± 1.76%.

DISCUSSION

Impaired endothelial-dependent FMD of conduit arteries is a characteristic feature of subjects with known vascular disease risk factors (22). In particular, several previous studies have demonstrated that cigarette smoking alone is sufficient to impair flow-mediated brachial artery dilation in otherwise healthy young adults (21). Both active and passive smoking are associated with dose-related and partially reversible endothelial dysfunction. However, so far it has been unclear which functional consequences cigarette smoking in young subjects may have on the central arteries in addition to the impairment of peripheral brachial artery reactivity.

We have extended these previous observations by investigating for the first time the effects of cigarette smoking on both peripheral endothelial function and on central vascular function. By applying noninvasive MRI with high temporal and spatial resolution, we were able to simultaneously demonstrate that the impairment in peripheral endothelial function is accompanied by a significant impairment of central vascular distensibility and marked changes of proximal aortic PWV.

Assessment of endothelial function. Most methods developed to date for studying endothelial function are focus-

ing on the endothelium's potential to release nitric oxide in response to either pharmacologic or physiologic stimuli. Coronary artery testing with quantitative angiography or Doppler wire measurements of coronary vasodilator response to intracoronary infusion of vasoactive agents such as acetylcholine have been used to define the role of endothelial dysfunction predisposing to dynamic plaque development and activation (23,24). In order to establish less invasive methods for measuring endothelial function in humans, peripheral arterial techniques have been devised. Systematic comparisons revealed a close correlation of endothelial function in the human coronary and peripheral circulations (25).

Previously, the consequences of chronic cigarette smoking in young adults have been investigated by using external ultrasound imaging with analysis of vessel diameter changes due to hyperemia and after nitrate application (21). In a study investigating 200 subjects, Celermajer et al. (21) demonstrated an inverse relation of flow-mediated brachial artery dilation and lifetime cigarette dose smoked. Even in the group of light smokers (defined as cigarette consumption up to 10 pack-years), they detected a reduction of FMD to 4% diameter change (vs. 10% in the control group). This compares closely with the present study, where MRI showed a significant reduction of FMD in the smoker group.

Brachial artery diameter measurements can be accurately performed using high-resolution ultrasound imaging (26). In a recent validation study, de Roos et al. (27) showed a correlation of variance of 0.05 for reading variation of brachial artery diameters at baseline and after cuff release, respectively. The coefficient of variability for intraobserver comparison of FMD was 0.34. In comparison, reproducibility analysis of magnetic resonance measurements in the present study revealed a similar coefficient of variability of 0.05 and 0.06 for brachial artery area measurements at baseline and after cuff release with a coefficient of variability of 0.32 for repeated FMD measurements.

Whereas the accuracy and reproducibility of ultrasound methods for quantifying brachial artery reactivity have been discussed controversially in previous studies (28,29), the ultrasound technique has significantly improved over the last years due to the development of new high-resolution ultrasound scanners and the use of state-of-the-art image analysis methods (30). Hence, by implementing and applying all these technical developments, ultrasound imaging can have a very high precision and technical reproducibility. The main advantage of magnetic resonance vascular imaging beyond allowing for accurate and reproducible quantitation is its potential to give a wide range of parameters from different vessel types in different territories. In our opinion, this is of additional value beyond the actual measurement precision, because the biggest variable in any of the measured vascular parameters is likely to be inherent biological variation. Hence, an "integrated phenotyping" approach may help in getting a more comprehensive view of the vascular pathophysiology than relying on one single parameter, however well one can measure it.

Pathophysiology of vascular compliance. In the present study, blood pressure recordings showed a similar mean blood pressure in both groups and only a slight increase of systolic and decrease of diastolic blood pressure in smokers compared with the controls. However, this constellation resulted in a significant augmentation of pulse pressure in the group of smokers (48 $\pm$ 4 mm Hg vs. control 39 $\pm$ 2 mm Hg; $p < 0.05$). Increased pulse pressure indicates increased arterial stiffness and is commonly seen in older subjects. Our results suggest that a dysfunctional endothelial system leads to a loss of hyperemia-induced brachial artery reactivity as well as to a significant reduction of arterial distensibility in the central vascular system. This was observed both in the common carotid arteries as well as at different sites of the aorta.

It was interesting to note that, in both the smokers and the control subjects, the absolute changes of cross-sectional area with every cardiac cycle were highest in the AA, followed by the proximal aorta, and finally the DDA. These large changes of cross-sectional area in the AA with every cardiac contraction are in good agreement with the physiologic Windkessel function of the proximal part of the thoracic aorta. However, when taking the vessel size of the aorta into account with a decrease of cross-sectional area from the proximal to the distal aorta, relative area change was decreasing along the course of the aorta both in smokers and in nonsmoking controls. This is in close agreement with a previous study by Resnick et al. (31) who also observed lower aortic distensibilities in the proximal descending aorta both in healthy volunteers and subjects with essential hypertension and increased aortic stiffness.

Relationship between conduit vessel stiffness and endothelial function. Factors that impair endothelial function are believed to be associated with increased arterial stiffness. The large conduit vessels possess a significant muscular component, which is partially under the control of the endothelium. Thus, changes in endothelial function can alter the mechanical properties of the large arteries and result in increased stiffness. Our study supports the findings of previous investigations where impairment of flow-mediated brachial artery dilation was associated with a marked decrease in aortic compliance (32,33). Furthermore, it was interesting to note that brachial artery (peripheral) distensibility was not significantly reduced in smokers ($p = 0.62$), whereas there were significant reductions of (central) aortic distensibility at all sites measured. One interpretation of these findings is that smoking-related endothelial dysfunction in the brachial artery verified by loss of FMD may have much less influence on the distensibility of the predominantly muscular brachial artery than it does on the distensibility of the more elastic aorta. Similarly, a population study looking at the effects of age on vascular stiffness in nearly 500 subjects reported an unchanged brachial artery

distensibility throughout all age groups, whereas there was a clear correlation between age and aortic distensibility (34).

Although arterial compliance and distensibility are regarded as indicators of arterial stiffness, the role of PWV as a marker of vascular stiffness is still controversial. Nigam et al. (33) reported only a weak correlation between flow-mediated brachial artery dilation and PWV determined by tonometry ($r = 0.25$). In a recent study in patients with syndrome X, there was a strong correlation of the degree of peripheral endothelial dysfunction and pulse-wave propagation ($r = 0.86$) with a high corresponding sensitivity and specificity of PWV for discrimination of patients with syndrome X and healthy controls (35). Interestingly, the present study revealed a significant increase in PWV in the proximal aorta (comprising the AA and aortic arch) in the smokers (+19%, $p = 0.02$), whereas PWV in more distal parts of the aorta was similar between smokers and control subjects ($p = 0.96$). These findings are in close agreement with data from previous magnetic resonance studies demonstrating mainly the involvement of the AA in the aging process (13). Rogers et al. (15) reported a significantly higher PWV in the aortic region spanning the AA and aortic arch than in the more distal parts of the aorta in volunteers >55 years old. In comparison, the younger group <55 years of age showed similar PWV at each aortic location. Furthermore, aortic pulse-wave velocities of control subjects evaluated in the present study (proximal aorta 4.41 ± 0.16 m/s, distal aorta 4.77 ± 0.32 m/s) agreed highly with Doppler ultrasound PWV quantifications in previous studies (e.g., Wildman et al. [36]) reporting a PWV of 4.68 m/s in 186 young adults with an age range of 20 to 40 years. In general, important advantages of the MRI-based quantification of PWV are the accurate assessment of path length of the pulse-wave propagation and the ability to measure PWV within more localized sections of the aorta and at central sites difficult to assess by ultrasound probes.

Study limitations. The main aim of this study was to investigate whether functional changes in the vascular system due to chronic smoking can be detected in a relatively small sample size using high-resolution MRI. Therefore, a group of young smokers without any confounding cardiovascular risk factors was compared with an age- and weight-matched control group of nonsmokers. Acute effects of cigarette smoking on the vascular system with observance of time course of functional changes were not investigated. However, previous studies demonstrate that cigarette smoking is associated with an acute impairment of microvascular function (37). Furthermore, Neunteufl et al. (38) showed that, even in long-term smokers, acute impairment of endothelial function can be provoked by the smoking of one single cigarette. The duration of the nicotine-induced endothelial dysfunction and the order and exact time course of changes in FMD and PWV is currently unclear and remains to be studied.

The PWV was calculated as the ratio of distance between aortic measurement levels and the delay time between arrival of the pulse wave at these defined levels. The "arrival time" of the pulse wave at these levels was considered when the mean velocity reached half of its maximum value, as suggested by previous studies (20). In general, the definition of exact time of arrival of the flow wave is difficult, as timing will vary depending on the curve algorithm one is using. An alternative way of magnetic resonance-derived measurement of aortic PWV is a method using the transit time of the foot of the flow wave across the aortic arch and the distance between the locations of both measurements. In this method initially described by Mohiaddin et al. (13), the foot of the ascending and descending aorta flow waves are estimated as the point of interception of the linear extrapolation of the steep early systolic slope and the late diastolic flow baseline. A potential source of error lies in the extrapolation of the steep upstroke of the curve and the definition of the baseline. However, MRI allows measurement of flow profiles with high temporal and spatial resolution. Hence, the flow curves are smoother than area curves because the blood velocity is low near the arterial wall, and the mean flow is, therefore, only slightly dependent on the sharpness of the aortic outline. This allows for curve fitting with walking average of at least four points for the upstroke limb flow curve. Validation studies revealed a high accuracy of magnetic-resonance-derived flow measurements based on phase-contrast techniques (39).

Conclusions. In the present magnetic resonance study, we were able to demonstrate that cigarette smoking in young and otherwise healthy volunteers results not only in a reduction of hyperemia-induced brachial artery reactivity but also in significant impairment of carotid and aortic compliance as well as in changes of central PWV. At present, measurements of arterial stiffness applying a variety of different techniques are mainly made for physiologic or experimental studies rather than clinical practice. However, it is likely that, over the next few years, measurements of arterial stiffness will become an increasingly important part of the process of risk assessment, and may possibly be valuable in monitoring new therapeutic strategies (40). Noninvasive MRI bears the potential for such detailed characterization of vascular function in one single examination and may play an important role both in research and in clinical practice by giving new insight into mechanisms involved in regulation of peripheral and central vascular function.

Reprint requests and correspondence: Dr. Frank Wiesmann, Medizinische Universitaetsklinik, Josef-Schneider-Str. 2, 97080 Würzburg, Germany. E-mail: f.wiesmann@mail.uni-wuerzburg.de.

REFERENCES

1. Ross R. Atherosclerosis—an inflammatory disease. N Engl J Med 1999;340:115–26.

2. Schachinger V, Britten MB, Zeiher AM. Prognostic impact of coronary vasodilator dysfunction on adverse long-term outcome of coronary heart disease. Circulation 2000;101:1899–906.
3. Halcox JP, Schenke WH, Zalos G, et al. Prognostic value of coronary vascular endothelial dysfunction. Circulation 2002;106:653–8.
4. Heitzer T, Schlinzig T, Krohn K, Meinertz T, Munzel T. Endothelial dysfunction, oxidative stress, and risk of cardiovascular events in patients with coronary artery disease. Circulation 2001;104:2673–8.
5. Perticone F, Ceravolo R, Pujia A, et al. Prognostic significance of endothelial dysfunction in hypertensive patients. Circulation 2001; 104:191–6.
6. Gokce N, Keaney JF, Jr., Hunter LM, Watkins MT, Menzoian JO, Vita JA. Risk stratification for postoperative cardiovascular events via noninvasive assessment of endothelial function: a prospective study. Circulation 2002;105:1567–72.
7. Glasser SP. On arterial physiology, pathophysiology of vascular compliance, and cardiovascular disease. Heart Dis 2000;2:375–9.
8. Cohn JN. Arterial compliance to stratify cardiovascular risk: more precision in therapeutic decision making. Am J Hypertens 2001;14: 258S–63S.
9. Oliver JJ, Webb DJ. Noninvasive assessment of arterial stiffness and risk of atherosclerotic events. Arterioscler Thromb Vasc Biol 2003;23: 554–66.
10. Biederman RW, Fuisz AR, Pohost GM. Magnetic resonance angiography. Curr Opin Cardiol 1998;13:430–7.
11. Riederer SJ, Bernstein MA, Breen JF, et al. Three-dimensional contrast-enhanced MR angiography with real-time fluoroscopic triggering: design specifications and technical reliability in 330 patient studies. Radiology 2000;215:584–93.
12. Wutke R, Lang W, Fellner C, et al. High-resolution, contrast-enhanced magnetic resonance angiography with elliptical centric k-space ordering of supra-aortic arteries compared with selective X-ray angiography. Stroke 2002;33:1522–9.
13. Mohiaddin RH, Firmin DN, Longmore DB. Age-related changes of human aortic flow wave velocity measured noninvasively by magnetic resonance imaging. J Appl Physiol 1993;74:492–7.
14. Mohiaddin RH, Underwood SR, Bogren HG, et al. Regional aortic compliance studied by magnetic resonance imaging: the effects of age, training, and coronary artery disease. Br Heart J 1989;62:90–6.
15. Rogers WJ, Hu YL, Coast D, et al. Age-associated changes in regional aortic pulse wave velocity. J Am Coll Cardiol 2001;38:1123–9.
16. Fayad ZA, Nahar T, Fallon JT, et al. In vivo magnetic resonance evaluation of atherosclerotic plaques in the human thoracic aorta: a comparison with transesophageal echocardiography. Circulation 2000; 101:2503–9.
17. Fayad ZA, Fuster V. Clinical imaging of the high-risk or vulnerable atherosclerotic plaque. Circ Res 2001;89:305–16.
18. Cai JM, Hatsukami TS, Ferguson MS, Small R, Polissar NL, Yuan C. Classification of human carotid atherosclerotic lesions with in vivo multicontrast magnetic resonance imaging. Circulation 2002;106: 1368–73.
19. Sorensen MB, Collins P, Ong PJ, et al. Long-term use of contraceptive depot medroxyprogesterone acetate in young women impairs arterial endothelial function assessed by cardiovascular magnetic resonance. Circulation 2002;106:1646–51.
20. Groenink M, de Roos A, Mulder BJ, Spaan JA, van der Wall EE. Changes in aortic distensibility and pulse wave velocity assessed with magnetic resonance imaging following beta-blocker therapy in the Marfan syndrome. Am J Cardiol 1998;82:203–8.
21. Celermajer DS, Sorensen KE, Georgakopoulos D, et al. Cigarette smoking is associated with dose-related and potentially reversible impairment of endothelium-dependent dilation in healthy young adults. Circulation 1993;88:2149–55.
22. Celermajer DS, Sorensen KE, Gooch VM, et al. Non-invasive detection of endothelial dysfunction in children and adults at risk of atherosclerosis. Lancet 1992;340:1111–5.
23. Ludmer PL, Selwyn AP, Shook TL, et al. Paradoxical vasoconstriction induced by acetylcholine in atherosclerotic coronary arteries. N Engl J Med 1986;315:1046–51.
24. Vita JA, Treasure CB, Nabel EG, et al. Coronary vasomotor response to acetylcholine relates to risk factors for coronary artery disease. Circulation 1990;81:491–7.
25. Anderson TJ, Uehata A, Gerhard MD, et al. Close relation of endothelial function in the human coronary and peripheral circulations. J Am Coll Cardiol 1995;26:1235–41.
26. Sorensen KE, Celermajer DS, Spiegelhalter DJ, et al. Non-invasive measurement of human endothelium dependent arterial responses: accuracy and reproducibility. Br Heart J 1995;74:247–53.
27. De Roos NM, Bots ML, Schouten EG, Katan MB. Within-subject variability of flow-mediated vasodilation of the brachial artery in healthy men and women: implications for experimental studies. Ultrasound Med Biol 2003;29:401–6.
28. Kobayashi H, Yoshida A, Kobayashi M, Nakao S. Non-invasive detection of endothelial dysfunction with 30 MHz transducer. Lancet 1996;347:1336–7.
29. Hardie KL, Kinlay S, Hardy DB, Wlodarczyk J, Silberberg JS, Fletcher PJ. Reproducibility of brachial ultrasonography and flow-mediated dilatation (FMD) for assessing endothelial function. Aust N Z J Med 1997;27:649–52.
30. Leeson CP, Hingorani AD, Mullen MJ, et al. Glu298Asp endothelial nitric oxide synthase gene polymorphism interacts with environmental and dietary factors to influence endothelial function. Circ Res 2002; 90:1153–8.
31. Resnick LM, Militianu D, Cunnings AJ, Pipe JG, Evelhoch JL, Soulen RL. Direct magnetic resonance determination of aortic distensibility in essential hypertension: relation to age, abdominal visceral fat, and in situ intracellular free magnesium. Hypertension 1997;30: 654–9.
32. Hirai T, Sasayama S, Kawasaki T, Yagi S. Stiffness of systemic arteries in patients with myocardial infarction: a noninvasive method to predict severity of coronary atherosclerosis. Circulation 1989;80:78–86.
33. Nigam A, Mitchell GF, Lambert J, Tardif JC. Relation between conduit vessel stiffness (assessed by tonometry) and endothelial function (assessed by flow-mediated dilatation) in patients with and without coronary heart disease. Am J Cardiol 2003;92:395–9.
34. van der Heijden-Spek JJ, Staessen JA, Fagard RH, Hoeks AP, Boudier HA, van Bortel LM. Effect of age on brachial artery wall properties differs from the aorta and is gender dependent: a population study. Hypertension 2000;35:637–42.
35. Kidawa M, Krzeminska-Pakula M, Peruga JZ, Kasprzak JD. Arterial dysfunction in syndrome X: results of arterial reactivity and pulse wave propagation tests. Heart 2003;89:422–6.
36. Wildman RP, Mackey RH, Bostom A, Thompson T, Sutton-Tyrrell K. Measures of obesity are associated with vascular stiffness in young and older adults. Hypertension 2003;42:468–73.
37. Ijzerman RG, Serne EH, van Weissenbruch MM, de Jongh RT, Stehouver CD. Cigarette smoking is associated with an acute impairment of microvascular function in humans. Clin Sci (Lond) 2003;104: 247–52.
38. Neunteufl T, Heher S, Kostner K, et al. Contribution of nicotine to acute endothelial dysfunction in long-term smokers. J Am Coll Cardiol 2002;39:251–6.
39. Bolster BD Jr., Atalar E, Hardy CJ, McVeigh ER. Accuracy of arterial pulse-wave velocity measurement using MR. J Magn Reson Imaging 1998;8:878–88.
40. Mackenzie IS, Wilkinson IB, Cockcroft JR. Assessment of arterial stiffness in clinical practice. QJM 2002;95:67–74.